이학석사 학위논문

Inhibition of angiogenesis in HUVECs by a novel cell-penetrating peptide-siVEGF complex

새로운 세포 투과 펩타이드−siVEGF 복합체를
이용한 인간 탯줄 정맥 내피세포의 혈관 신생 억제

2023 년 8 월

서울대학교 대학원
자연과학대학 협동과정 유전공학 전공

김 민 서

Inhibition of angiogenesis in HUVECs by a novel cell-penetrating peptide-siVEGF complex

지도교수 노 상 호

이 논문을 이학석사 학위논문으로 제출함

2023 년 6 월

서울대학교 대학원

자연과학대학 협동과정 유전공학 전공

김 민 서

김 민 서의 이학석사 학위논문을 인준함

2023 년 6 월

위 원 장	백 정 화	(인)
부위원장	노 상 호	(인)
위 원	박 한 검	(인)

ABSTRACT

Inhibition of angiogenesis in HUVECs by a novel cell-penetrating peptide-siVEGF complex

Minseo Kim

Interdisciplinary Graduate Program in Genetic Engineering

The Graduate School

Seoul National University

(Directed by Prof. Sangho Roh, D.V.M., Ph.D)

Angiogenesis, mediated by vascular endothelial growth factor (VEGF), plays a key role in wound healing, inflammatory diseases, cardiovascular processes, ocular diseases and, in particular, tumor growth. Therefore, modulation of angiogenesis is a promising candidate for the treatment of the disease, and therapeutic approaches targeting VEGF and its receptors have been widely investigated. RNA interference is a powerful tool for treating diseases, but its application has been restricted by the lack of efficient small interfering RNA (siRNA) delivery systems. The purpose of this study was to demonstrate that an amphipathic cell-penetrating peptide, Ara27, is an

effective VEGF siRNA (siVEGF) delivery vehicle by complexing with siVEGF.

Without cytotoxicity, the Ara27-siVEGF complex provided effective siVEGF delivery to human umbilical vein endothelial cells (HUVECs) and specifically downregulates both the mRNA and protein levels of VEGF. Furthermore, wound healing and tube formation in HUVECs, which can be an indicator of angiogenesis, were inhibited by the Ara27-siVEGF complex through attenuating the phosphorylation of VEGFR2, AKT and ERK in HUVECs. Therefore, angiogenesis in HUVECs was inhibited by a novel cell-penetrating peptide-siVEGF complex. Collectively, these results present that Ara27 is a potential candidate for efficient siRNA delivery without significant cytotoxicity.

Keywords: Angiogenesis, cell-penetrating peptide, VEGF siRNA, HUVEC, Drug delivery system

Student Number: 2021-29018

CONTENTS

ABSTRACT i

CONTENTS iii

LIST OF FIGURES iv

LIST OF TABLES v

ABBREVIATIONS vi

INTRODUCTION 1

MATERIALS AND METHODS 4

RESULTS 16

DISCUSSION 34

REFERENCES 39

국문초록 46

LIST OF FIGURES

Figure 1. Electrophoretic mobility shift assay to determine the optimal molar ratio for CPP-siVEGF complex formation.

Figure 2. Size distribution the CPP-siVEGF complexes at various charge ratios using Zetasizer.

Figure 3. HUVEC viability measured by WST assay under various treatment conditions.

Figure 4. Efficiency of cellular uptake of siVEGF in HUVECs using confocal microscopy.

Figure 5. Gene silencing efficiency in HUVEC following siVEGF transfection using TransITx2.

Figure 6. Gene silencing efficiency in HUVEC following siVEGF transfection using Ara27-siVEGF complex.

Figure 7. Wound healing assay and quantitative analysis of wound healing area after 48h of treatments.

Figure 8. Effect of Ara27-siVEGF complex on HUVEC tube formation assay.

Figure 9. The protein expression of VEGF/VEGFR2/ERK/AKT signaling pathway after 48 h treatments.

Figure 10. Schema illustrating the mechanism of angiogenesis inhibition in HUVECs by a novel CPP-siVEGF complex.

LIST OF TABLES

Table 1. Sequence information of the siRNAs used in this study

Table 2. Fluorescence wavelengths information used in confocal microscopy

Table 3. Sequence information of the primer used in this study

Table 4. Size and polydispersity index of Ara27-siVEGF complex

ABBREVIATIONS

CPP	Cell Penetrating Peptide
siRNA	short interfering RNA
HUVEC	Human Umbilical Vein Endothelial Cell
VEGF	Vascular Endothelial Growth Factor
siVEGF	Vascular Endothelial Growth Factor siRNA
siNC	Negative Control siRNA
GAPDH	Glyceraldehyde 3-phosphate dehydrogenase
PBS	Phosphate-buffered saline
RT-qPCR	Quantitative real-time reverse ` transcription-polymerase chain reaction
BSA	Bovine Serum Albumin
TBS	Tris-Buffered Saline

INTRODUCTION

Angiogenesis is the process of new blood vessels forming by expansion of the surrounding vascular network [1]. Thus, angiogenesis is essential for growth and development and plays a key role in wound healing, inflammatory diseases, cardiovascular processes, ocular diseases and, in particular, tumor growth and metastasis [2-4]. Angiogenesis is regulated by pro- and anti-angiogenic factors, and changes in this equilibrium can activate the angiogenic switch, leading to pathological vessel formation [5]. Vascular Endothelial Growth Factor (VEGF) is one of the major pro-angiogenic molecules, stimulating endothelial cell proliferation, migration and neovascularization through crosstalk with VEGF receptor-2 [6]. Because of these critical functions, drugs have been developed to modulate angiogenesis by targeting VEGF and its receptors. Some of these drugs are in clinical use, including monoclonal antibodies, small molecule tyrosine kinase inhibitors, and molecular inhibitors of signaling pathways [7-9]. However, these drugs must be administered at high doses to maintain sufficient drug effects, which can lead to non-specific binding, unexpected toxicities, and side effects [10-12]. Therefore, the development of novel anti-angiogenic agents with high efficacy and low toxicity is imperative.

RNA interference (RNAi) is emerging as a promising therapeutic approach to modulating gene expression by sequence-specific mRNA degradation [13, 14]. Small interfering RNA (siRNA), due to its significant effects, high

specificity and low side effects, has been explored as a potential gene therapy for the treatment of various classes of inherited and acquired diseases [15-17]. However, delivering siRNA is still challenging due to its pharmacological properties. The phosphate groups on their surfaces make them difficult to diffuse across cellular membranes because they are highly anionic [18]. In the past several years, diverse vectors have been explored to improve siRNA pharmacokinetics, cellular delivery, and intracellular trafficking [19, 20]. However, viral vectors are restricted from clinical applications due to the concerns of strong immunogenicity, high toxicity, and inflammatory reactions, while non-viral carriers are becoming promising therapeutic nucleic acid delivery tools because of their biocompatibility and physicochemical properties [21].

Cell-penetrating peptide (CPP) is defined as a short (~5-30 amino acids) peptide that has cell membrane protein transduction domains or membrane translocating sequences [22]. They are comprised of cationic or amphipathic sequences that can cross the cell membranes [23]. The CPPs can deliver various kinds of cargo into cell cytosols, such as fluorophores, drugs, peptides and nucleic acids [24-26]. By interacting noncovalently with CPP, siRNA can be delivered by forming complexes with the cationic part and anionic part of CPP [27, 28]. However, when cationic CPPs were masked their cationic charges by nucleic acid, it is less efficient for CPP-siRNA complex to be taken up into cells [29]. Compared to cationic CPPs, amphipathic CPPs have greater

cellular uptake, cytosolic localization, endosomal escape properties and gene silencing effects [30-33]. Ara27, an amphipathic CPP, is confirmed internalization at low concentrations under short treatment conditions in various cell lines without cytotoxicity [34]. A significant improvement in intracellular uptake was shown with Ara27 as compared to commonly used CPPs, such as Tat-protein transduction domain and membrane translocating sequence, without adverse effects on the viability of the cells [35].

In this study, the Ara27-siVEGF complex was formed through noncovalent interaction and then characterized by electrophoretic mobility shift assay and size analysis. The complexes successfully delivered siVEGF to HUVEC cytosol without cytotoxicity. The VEGF mRNA and protein expression were downregulated following siVEGF delivery by complexes. Moreover, inhibition of angiogenesis was confirmed by wound healing and tube formation in HUVECs through inhibiting the AKT and ERK signaling pathways.

MATERIALS AND METHODS

2.1. Materials

Ara27, an amphipathic cell penetrating peptide (CPP), was synthesized by LifeTein (LifeTein LLC, NJ, USA) using PeptideSyn technology based on FMOC (9-fluorenylmethoxy carbonyl) chemistry. Ara27 was labeled with fluorescein isothiocyanate (FITC). The siRNA oligos used in this study were synthesized by Bioneer (Daejon, Korea). The sequences of the negative control siRNA (siNC) and VEGF siRNA (siVEGF) are shown in **Table 1**. The siVEGF sequence is referenced in previous studies [36-38] . Cyanine3 (Cy3) labeled siVEGF was also synthesized by Bioneer. TransITx2 was purchased from Mirus Bio (WI, USA) for using as positive control on transfection. Axitinib was obtained from Selleckchem (TX, USA).

Table 1. Sequence information of the siRNAs used in this study

Name	Sequence (5′to 3′)
si*VEGF*	**Sense: AUG UGA AUG CAG ACC AAA GA TT**
	Antisense: UUC UUG GUC UGC AUU CAC AU TT
si*NC*	**Sense: UUC UCC GAA CGU GUC ACG U TT**
	Antisense: ACG UGA CAC GUU CGG AGA A TT

2.2. Preparation of CPP-siVEGF complex

As a constant concentration of siVEGF (final concentration 50 nM), the Ara27 and siVEGF were mixed in different molar ratios (siVEGF : Ara27 = 1:1, 1:5, 1:10, 1:20 and 1:30). The Ara27-siVEGF complexes for *in vitro* experiment were prepared in PBS based 5% glucose solution and incubated at 37 °C for 30 min.

2.3. Electrophoretic mobility shift assay

Agarose gel electrophoresis assay was designed to determine siRNA binding affinity to Ara27. The CPP-siVEGF complexes were formed at different molar ratios (siVEGF : Ara27 = 1:1, 1:5, 1:10, 1:20 and 1:30) with a constant amount of 100 pmol of siRNA. After incubation for 30 min at 37 °C, the complexes mixed with a 6× loading dye were loaded into 2% (w/v) agarose gel dissolved in 100 mL of TAE buffer. The 2% agarose gel was electrophoresed at 70 V for 40 min in TAE buffer. The images of the electrophoretic mobility shift of the complexes were taken by the InGenius System (Syngene, Cambridge, UK).

2.4. Characterization of CPP-siVEGF complexes

Ara27-siVEGF complexes were measured by dynamic light scattering (Zetasizer Ultra; Malvern Instruments, Worcestershire, UK) in terms of mean size (Z-average) of the particle distribution and of homogeneity (PDI). The complexes were prepared as mentioned above.

2.5. Cell Culture

Human umbilical vein endothelial cells (HUVECs) were obtained from Promocell (Heidelberg, Germany). The HUVECs were cultured in Endothelial Cell Growth Medium (Promocell) and incubated at 37°C in a humidified atmosphere with 5% CO_2. HUVEC passages 4 to 9 were used for all experiments.

2.6. Cell Viability Assay

Cell viability was measured using the Cell Counting Kit-8 (CCK-8; Abbkine, Wuhan, China) based on water-soluble tetrazolium salt (WST-8). HUVECs were seeded at a density of 4000 cells/well on 96-well plates. After 24 h, the cells were treated under different conditions and incubated at 37°C. After 24 h of treatment, the medium was changed with fresh medium containing 10 μl of CCK-8 reagents and incubated at 37°C for 1 h. The absorbance was measured at 452 nm using a microplate reader (MikroskanTM GO Microplate Spectrophotometer; Thermo Fisher Scientific, MA, USA).

2.7. Cellular internalization observed using confocal microscopy

HUVECs were seeded on gelatin-coated coverslips at an appropriate density. After 24 h of stabilization, the cells were treated with Ara27-FITC 1 μM, siVEGF-cy3 50 nM, TransITx2 siVEGF-cy3 50 nM, and Ara27-siVEGF complex. After 24 h treatment, immunofluorescence staining was conducted. Briefly, cells on coverslips were washed three times with heparin-containing PBS and fixed for 10 min with 4% paraformaldehyde. Afterward, the coverslips were rinsed thoroughly with PBS and mounted on slides using a mounting solution containing Hoechst 33342. LSM800 confocal microscopy (Zeiss, Munich, Germany) was used to analyze all slide. Ara27 was labeled with FITC at C-terminal and siVEGF was labeled with Cy3 at 5′-end of sense ssRNA. The fluorescence wavelengths information is shown in **Table 2.**

Table2. Fluorescence wavelengths information used in confocal microscopy

	Hoechst	**FITC**	**Cy3**
Channel color	Blue	Green	Red
Excitation wavelength (nm)	353	495	548
Emission wavelength (nm)	465	519	561

2.8. Gene knockdown evaluation by RT-qPCR

A TaKaRa MiniBEST Universal RNA Extraction Kit (Takara, Tokyo, Japan) was used to isolate total RNA from cultured cells, followed by transcription to first-strand complementary DNA. RT-qPCR reactions were performed using a 7500 real-time PCR system (Applied Biosystems, CA, USA). The ΔΔCT method was employed to calculate relative expression. The expression of target mRNA was adjusted to that of internal control glyceraldehyde 3-phosphate dehydrogenase (GAPDH) in the same sample. Each value represents the average of three independently performed runs with standard deviations. The details of genes and their primer sequences are shown in **Table 3**.

Table 3. Sequence information of the primer used in this study

Gene	Primer sequence (5' to 3')
VEGF	**Forward: GCAGCTTGAGTTAAACGAACG**
	Reverse: GGTTCCCGAAACCCTGAG
GAPDH	**Forward: TGGACTCCACGACGTACTCA**
	Reverse: ACATGTTCCAATATGATTCC

2.9. Western Blot analysis.

Cells were lysed with cell lysis buffer for 30 min on ice and then centrifuged at 13,000g for 15 min at 4°C to clear the lysates. After removing debris by centrifugation, the supernatants were used for Western blot analysis. The protein concentrations were detected using a BCA protein assay kit (#23225, Thermo Fisher Scientific). Totals of 20 ~ 30 μg proteins were loaded and separated on an 8%-12% gradient on SDS-PAGE and then transferred onto PVDF membrane (Millipore, MA, USA). The membranes were blocked with 5% BSA (BD Bioscience, CA, USA) in TBST buffer and incubated overnight at 4°C with primary antibodies to VEGF (#SC7269, 1:1000; Santa Cruz, CA, USA), GAPDH (#ABL1020, 1:2000; Abbkine, CA, USA), VEGFR2 (#2479, 1:1000), p-VEGFR2 (#2478, 1:1000), AKT(#9272, 1:1000), p-AKT (#4060, 1:1000), ERK (#9102, 1:1000) and p-ERK (#4379, 1:1000; Cell Signaling Technology, MA, USA) and then, with horseradish peroxidase (HRP)- conjugated secondary antibody (GeneTex, MA, USA) for 1h at room temperature. Electrochemiluminescence reagents (#DG-WPAL250, DoGenBio, Seoul, Korea) were used to detect protein bands. The proteins were then visualized on a Fusion FX6.0 (Vilber Lourmat, Collégien, France) and images were analyzed using the Image J software (version 2.9). GAPDH was used to confirm that equal amounts of protein were loaded and transferred.

2.10. Wound healing assay

The cell migration assay was performed using a scratch wound healing assay. Briefly, HUVECs were seeded at 10^5 cells/well in a 12-well plate. After 24 h stabilization, the cells were scratched using pipette tips. Following scratching, the cells were washed with PBS, treated under various conditions and incubated at 37 °C and 5% CO_2 for 48 h. The phase contrast images were taken by EVOS XL Core (Thermo Fisher Scientific). The wound healing area and the percentage of wound healing were quantified by Image J software (version 2.9).

2.11. Tube formation assay

The tube formation assay was conducted on Cultrex Reduced Growth Factor Basement Membrane Extract (BME; R&D Systems, MN, USA) added to a 96-well plate at a volume of 50 µl/well and allowed to polymerize for 30 min at 37°C. After polymerization, HUVECs were seeded onto BME at 1.5×10^4 cells/well in 100 µl medium with or without reagents. The cells were incubated at 37°C in a 5% CO_2 incubator. The tube formation was observed under an inverted microscope after 24 h. Images were captured with EVOS XL Core (Thermo Fisher Scientific). The images were analyzed for the number of nodes, number of junctions and total sprout length and the quantification was performed using the "Angiogenesis analyzer" plug-in [39] in Image J software (version 2.9).

2.12. Statistical Analysis

All analyzes were performed using GraphPad Prism 5 software. Data were analyzed using analysis of variance (ANOVA) and presented as the mean ± SEM.

RESULTS

3.1. Preparation and characterization of CPP-siVEGF complexes

To effectively deliver siVEGF to HUVECs, Ara27 was complexed with siVEGF at various molar ratios. A mobility shift assay was performed on agarose gel electrophoresis to determine the formation and optimal ratio of the CPP-siVEGF complex. Up to a molar ratio of siVEGF:Ara27 of 1:5, the complex was incompletely formed and siVEGF bands remained at the bottom of the gel. In contrast, siVEGF bands at the bottom of the gel disappeared due to complex formation with Ara27 and adhered to the comb at ratios of 1:10, 20, and 30 **(Figure 1)**. In addition, the molecular size of the 1:10, 20, and 30 complexes was measured using the Zetasizer. The mean sizes of the complexes were 158.6 nm, 179.5 nm and 233.7 nm for 1:10, 1:20 and 1:30, respectively **(Figure 2, Table 4)**.

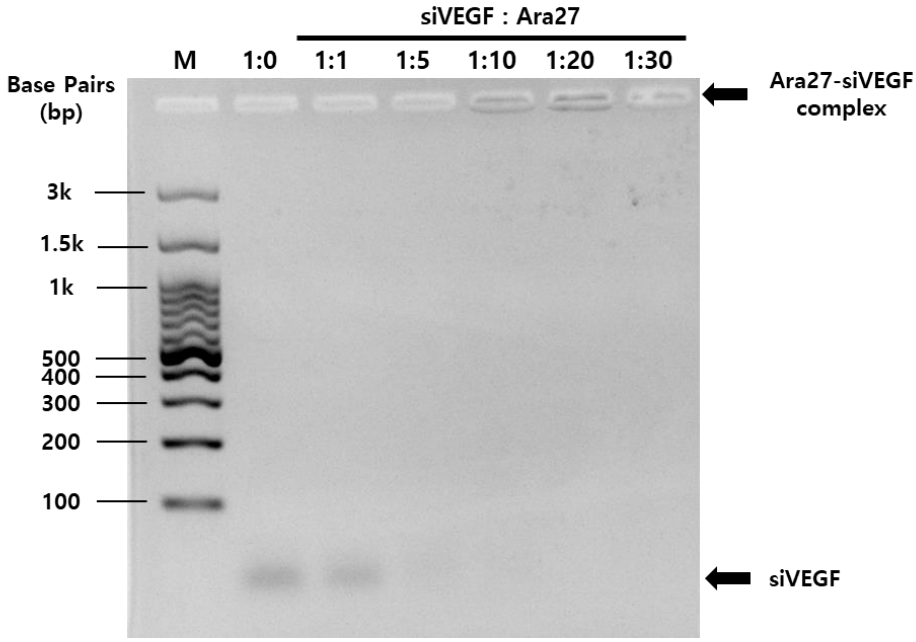

Figure 1. Electrophoretic mobility shift assay to determine the optimal molar ratio for CPP-siVEGF complex formation. The 21-bp siVEGF was mixed with Ara27 at molar ratios of 1:1, 1:5, 1:10, 1:20 and 1:30. The brightness and contrast of the picture were adjusted.

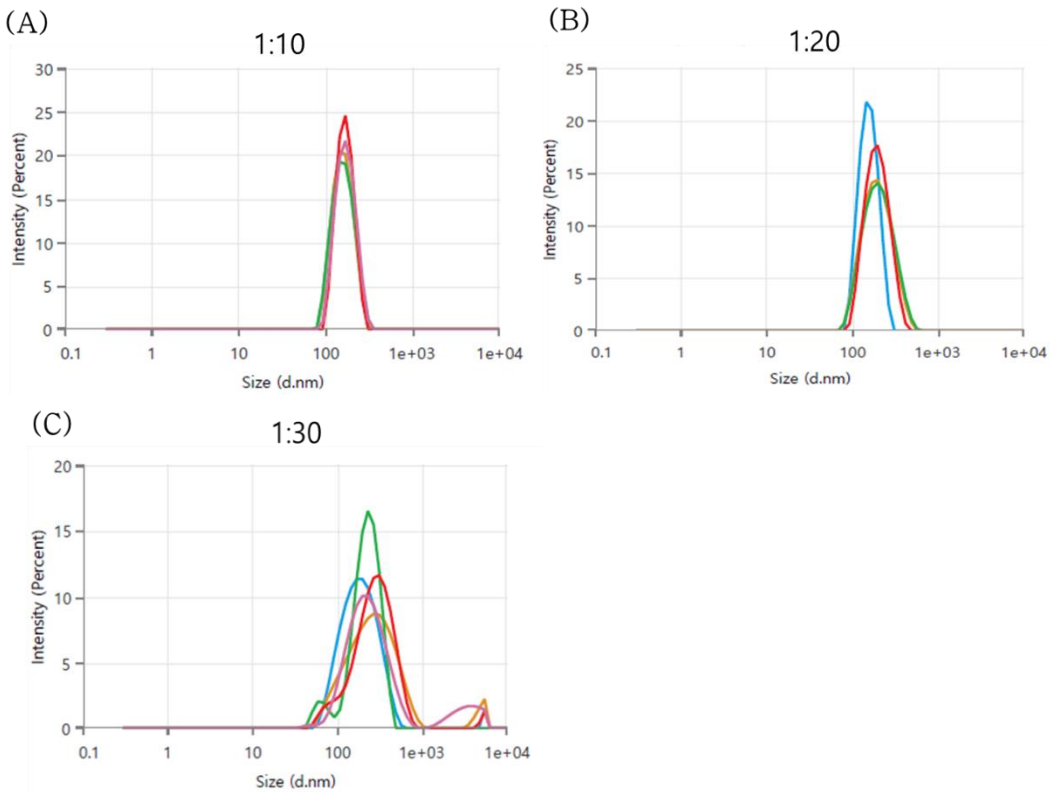

Figure 2. Size distribution the CPP-siVEGF complexes at various charge ratios using Zetasizer. The molar ratios of siVEGF: Ara27 were (A) 1:10, (B) 1:20, and (C) 1:30 with a final siVEGF concentration of 50 nM in all experiments.

Table 4. Size and polydispersity index of Ara27-siVEGF complex

siVEGF : Ara 27 (molar ratio)	Mean Complex size (nm)	Polydispersity Index
1:10	158.6	0.0630
1:20	179.5	0.1425
1:30	233.7	0.3536

3.2. Cytotoxicity of the CPP-siVEGF complex

To determine whether the complex induced toxicity in HUVECs prior to transfection, a WST assay was performed under various treatment conditions. First, Ara27, the amphipathic CPP used for complex formation, was not cytotoxic to HUVECs up to 1 μM after 24 h treatment **(Figure 3A)**. TransITx2, a commercial polymeric transfection reagent widely used as a positive control for transfection, showed cytotoxicity after a single treatment. Transfection with commercial transfection reagent was significantly cytotoxic, while siNC and siVEGF alone were not. In contrast, HUVECs maintained more than 90% viability when transfected with siNC and siVEGF via forming complexes with Ara27 **(Figure 3B)**. Overall, the Ara27-siVEGF complex appears to be the most effective candidate to inhibit HUVEC angiogenesis by intracellular siVEGF delivery.

(A)

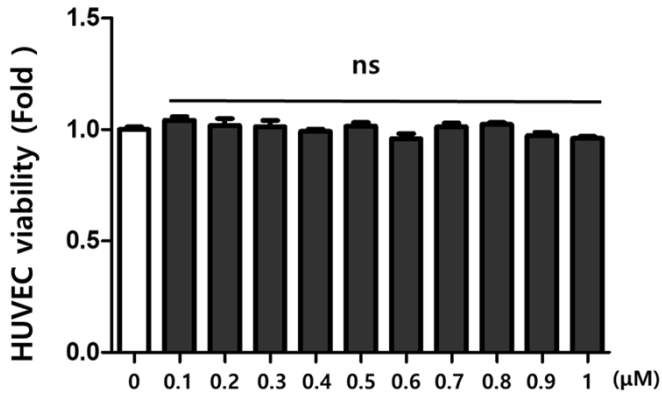

(B)

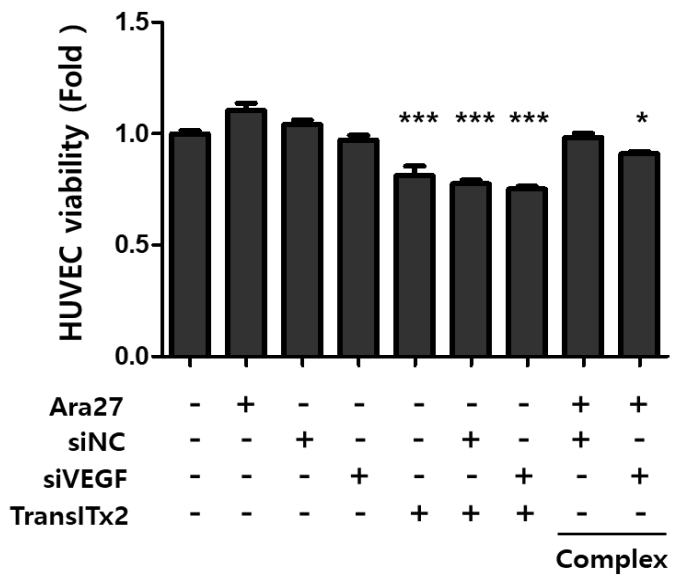

Figure 3. HUVEC viability measured by WST assay under various treatment conditions. (A) Viability of HUVEC according to the concentration of Ara27 for 24 h treatment. (B) Viability of HUVEC according to various treatment conditions. (n=3, **P* <0.05*;* ***P* < 0.01; ****P* < 0.001)

3.3. Intracellular uptake of CPP-siVEGF complex

Confocal microscopy observed cellular uptake of the CPP-siVEGF complex in HUVECs after treatment for 24 hours **(Figure 4)**. There are three images representing a red fluorescence of Cy3-labeled siVEGF, FITC-labeled Ara27 with green fluorescence, and a blue fluorescence of the nucleus. The intracellular localization of siVEGF was observed in both TransITx2 and Ara27-siVEGF complexes in HUVECs. These results indicate that Ara27 successfully delivered siVEGF into HUVEC cytosol. Furthermore, overlapping fluorescence in the merged image confirmed the co-localization of Cy3-labeled siVEGF and FITC-labeled Ara27.

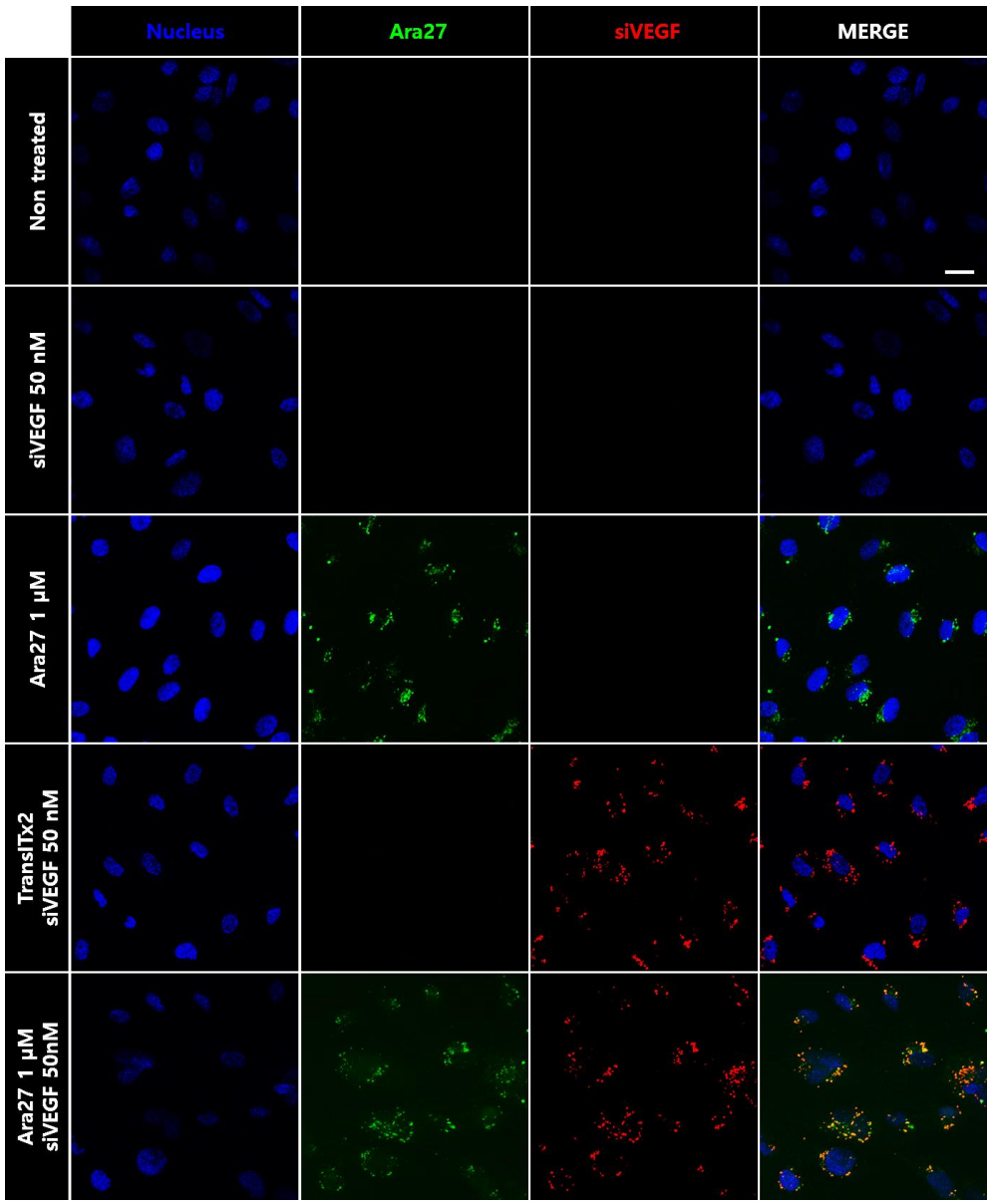

Figure 4. Efficiency of cellular uptake of siVEGF in HUVECs using confocal microscopy. HUVECs were treated different conditions for 24 h (non-treated, siVEGF-cy3 50 nM, Ara27-FITC 1 μM, TranITx2 siVEGF 50 nM and Ara27 1 μM + siVEGF 50 nM complex, respectively) and nucleus were counterstained with Hoechst 33342 for confocal laser scanning microscopy observation (scale bar = 20 μm)

3.4. *In vitro* VEGF silencing effect of CPP-siVEGF complex

As a positive control, HUVECs were transfected with siVEGF via TransITx2 before the CPP-siVEGF complex was used to assess the knockdown effect of VEGF. An RT-qPCR was used to analyze the expression of VEGF mRNA in HUVECs, and Western blot was used to assess the expression of VEGF protein in HUVECs. Compared to non-treated and siNC transfected HUVECs by transfection reagent, siVEGF transfected HUVECs showed effective downregulation of VEGF mRNA and protein levels **(Figure 5)**. Then, the CPP-siVEGF complex mediated knockdown of VEGF mRNA expression in HUVECs was analyzed by RT-qPCR. As expected, VEGF knockdown was clearly observed at Ara27-siVEGF complex. The Ara27-siVEGF complex reduced VEGF mRNA expression by almost 30%, similar to TransITx2 **(Figure 6A)**. In parallel, VEGF protein expression was also significantly downregulated by siVEGF delivery via the complex **(Figure 6B)**. These results indicate that the Ara27-siVEGF complex is nontoxic to HUVEC during effective intracellular siVEGF delivery, decreasing VEGF mRNA and protein expression.

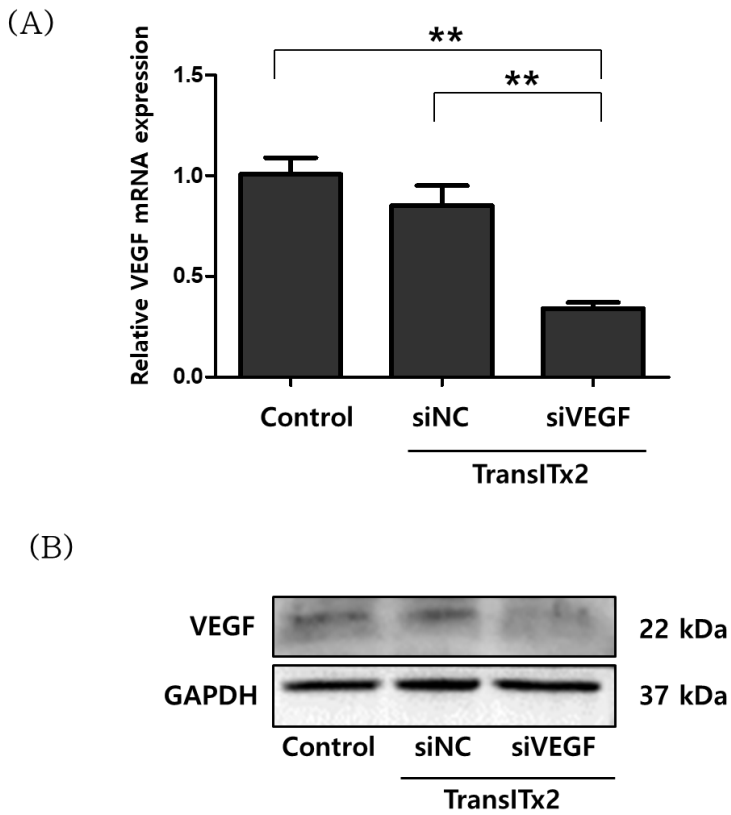

Figure 5. Gene silencing efficiency in HUVEC following siVEGF transfection using TransITx2. (A) The VEGF mRNA expression after treatment for 24 h. Relative VEGF mRNA were assessed by RT-qPCR using GAPDH for normalization. Statistical differences were calculated against control (n=3, $^{**}P < 0.01$). (B) The VEGF protein expression after 48 h treatment was examined by western blot. (siNC and siVEGF 50 nM)

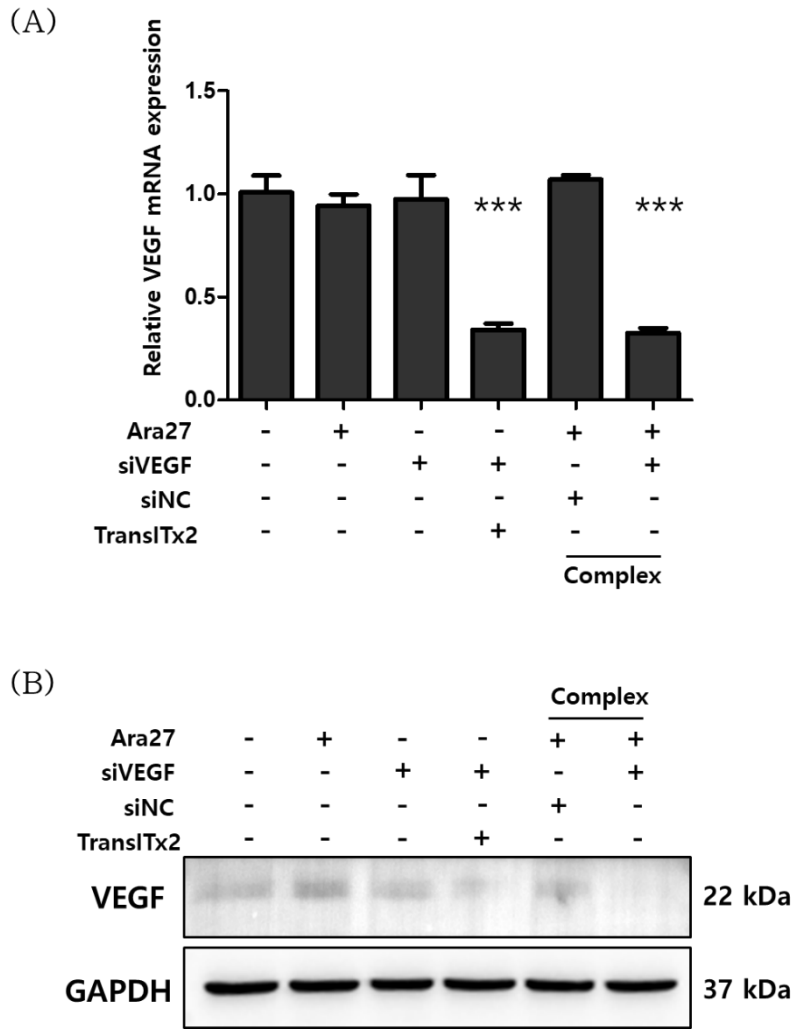

Figure 6. Gene silencing efficiency in HUVEC following siVEGF transfection using Ara27-siVEGF complex. (A) VEGF mRNA expression after treatment for 24 h (Ara27 1 μM, siVEGF 50 nM, TranITx2 siVEGF 50 nM, Ara27 1 μM + siNC 50 nM and Ara27 1 μM + siVEGF 50 nM complex, respectively). Relative VEGF mRNA were assessed by RT-qPCR using GAPDH for normalization. Statistical differences were calculated against control. (B) The VEGF protein expression after 48 h treatment was examined by western blot. GAPDH was used as a housekeeping control. (n=3, ***$P <$ 0.001)

3.5. Inhibition of angiogenesis in HUVECs by CPP-siVEGF complex via VEGF/VEGFR2-mediated AKT and ERK signaling pathways

The inhibitory effect of Ara27-siVEGF complex on angiogenesis was systematically evaluated based on high cell viability, siVEGF loading capacity and downregulated VEGF expression. First, a scratch wound healing assay was conducted to evaluate HUVEC migration activity, considering the importance of endothelial cell mobility during angiogenesis. Cell migration was inhibited upon treatment with TransITx2 and Ara27-siVEGF complex. The percentage of HUVEC migration was reduced to less than 20% in both transfection groups, while the migration of non-treated HUVEC was about 40% after 48 h incubation **(Figure 7)**. Subsequently, the angiogenic properties of HUVECs treated with different conditions were evaluated by in vitro tube formation assay on BME after 24 h incubation. Axitinib, an inhibitor of the VEGF receptor, was used as a positive control in the tube formation assay. Compared to the control groups, HUVECs treated with Ara27-siVEGF exhibited inhibited tube networks with fewer number of nodes, junctions and meshes **(Figure 8)**.

VEGF receptor-2 (VEGFR2) is considered to exhibit a major role in VEGF-mediated angiogenesis. Several downstream protein kinase pathways such as the RAF/MEK/ERK and PI3K/AKT pathways are closely involved in endothelial cell proliferation, cell survival and migration that can modulate

angiogenesis. Protein expression changes in the predicted pathways were evaluated by western blot to determine the signaling pathways associated with siVEGF delivery **(Figure 9)**. Decreased protein levels of p-VEGFR2, p-AKT and p-ERK were observed in HUVECs transfected with both TransITx2 and the Ara27-siVEGF complex. In particular, compared to a transfection reagent, the Ara27-siVEGF complex was more effective at inhibiting VEGFR2, AKT and ERK phosphorylation. In summary, these results indicate that a VEGF/VEGFR2/AKT/ERK signaling pathway is involved in the inhibition of angiogenesis in HUVECs.

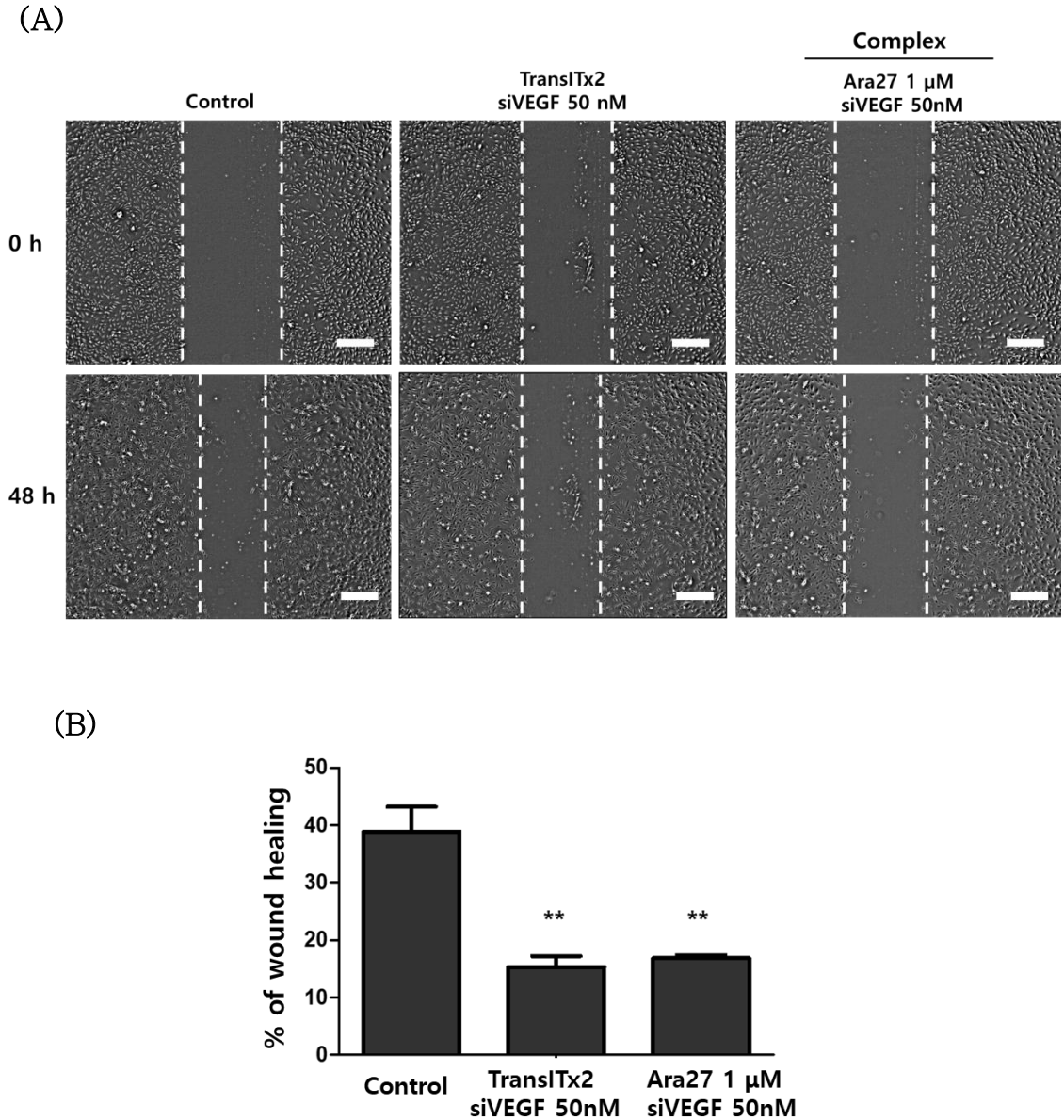

Figure 7. Wound healing assay and quantitative analysis of wound healing area after 48h of treatments. (A) Representative migration images of HUVECs at different time points (0, and 48 h) of different groups. (scale bar: 50 μm) (B) Quantitation of migration ability by calculating percentage of wound healing area (n=3, $^{**}P < 0.01$).

(A)

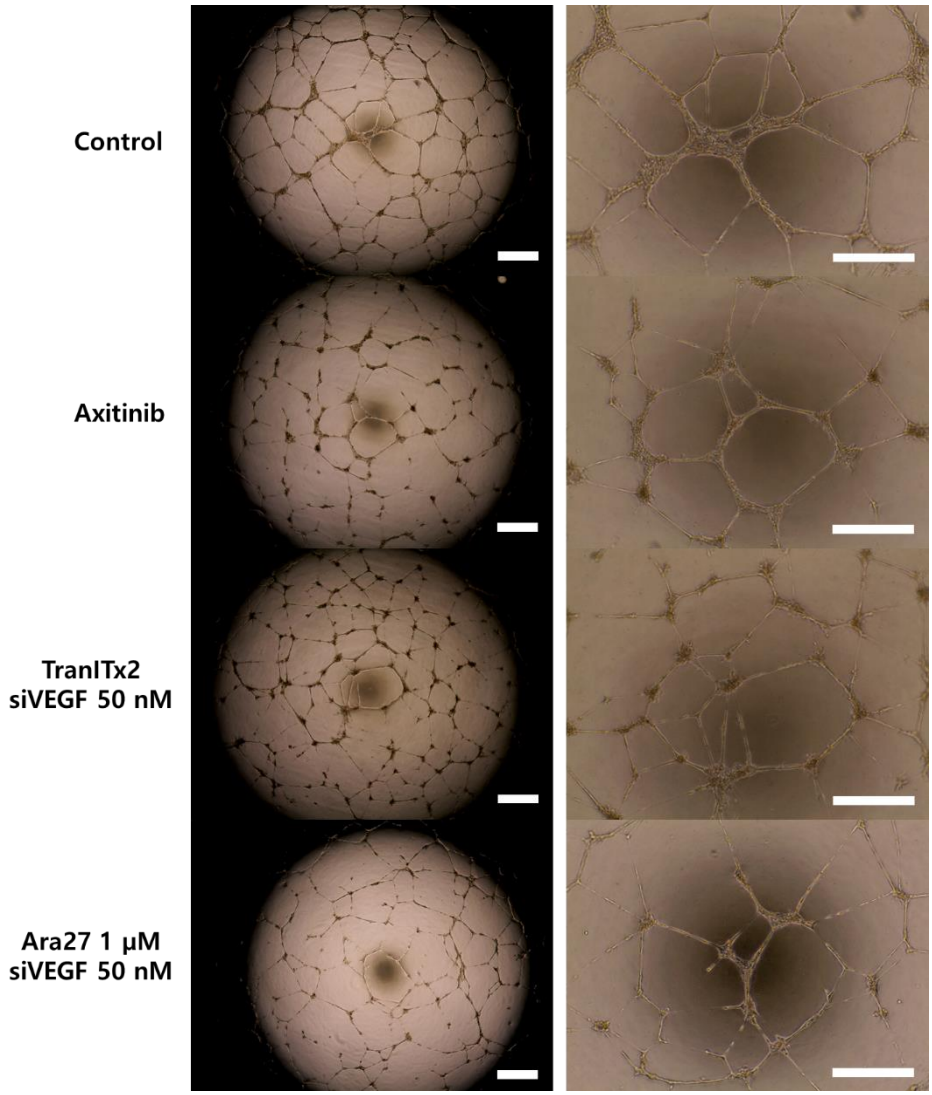
Control
Axitinib
TranITx2
siVEGF 50 nM
Ara27 1 μM
siVEGF 50 nM

(B)

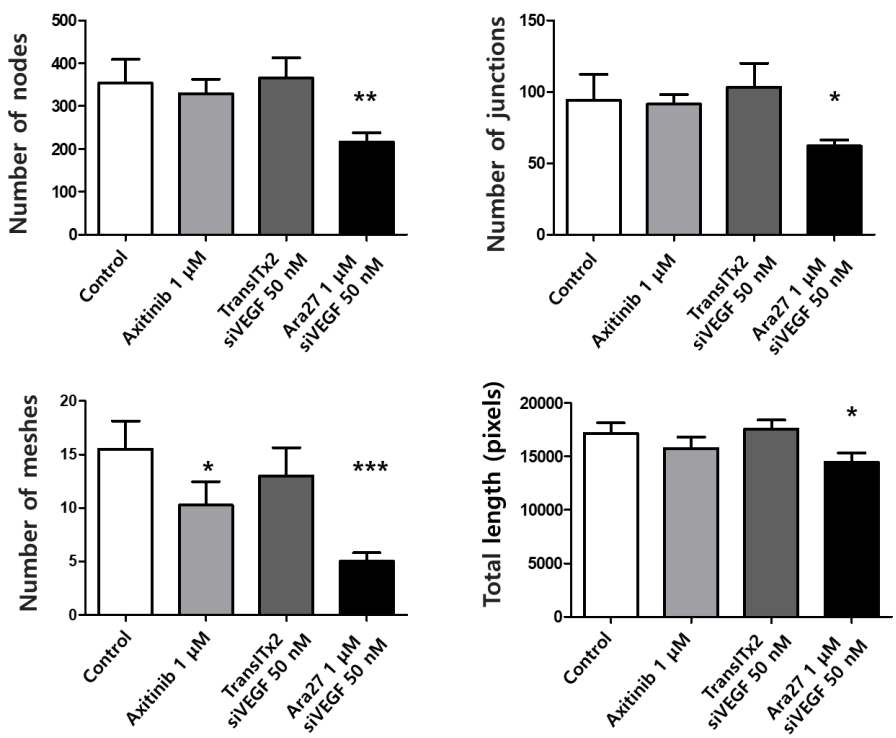

Figure 8. Effect of Ara27-siVEGF complex on HUVEC tube formation assay. (A) Representative images of HUVECs after 24 h of treatments. (scale bar: 50 μm) (B) Quantitative analyzes of the total nodes, junctions, meshes and length using Image J (n=3, $*P < 0.05$; $**P < 0.01$; $***P < 0.001$).

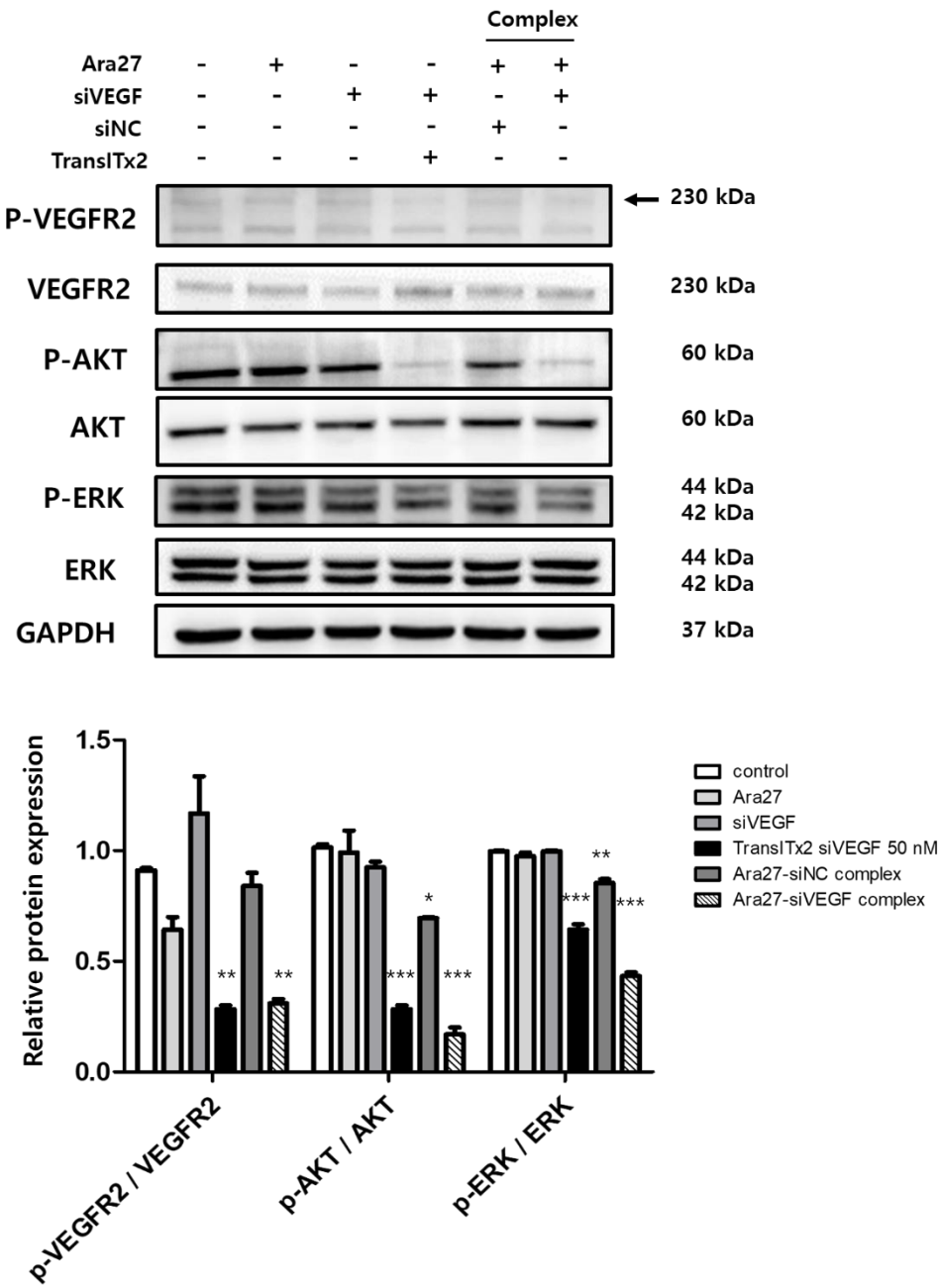

Figure 9. The protein expression of VEGF/VEGFR2/ERK/AKT signaling pathway after 48 h treatments. GAPDH was used as a housekeeping control. Ara27 1 μM, siVEGF 50 nM, TranITx2 siVEGF 50 nM, Ara27 1 μM + siNC 50 nM and Ara27 1 μM + siVEGF 50 nM complex, respectively. (n=3, **P* <0.05*;* ***P* < 0.01; ****P* < 0.001)

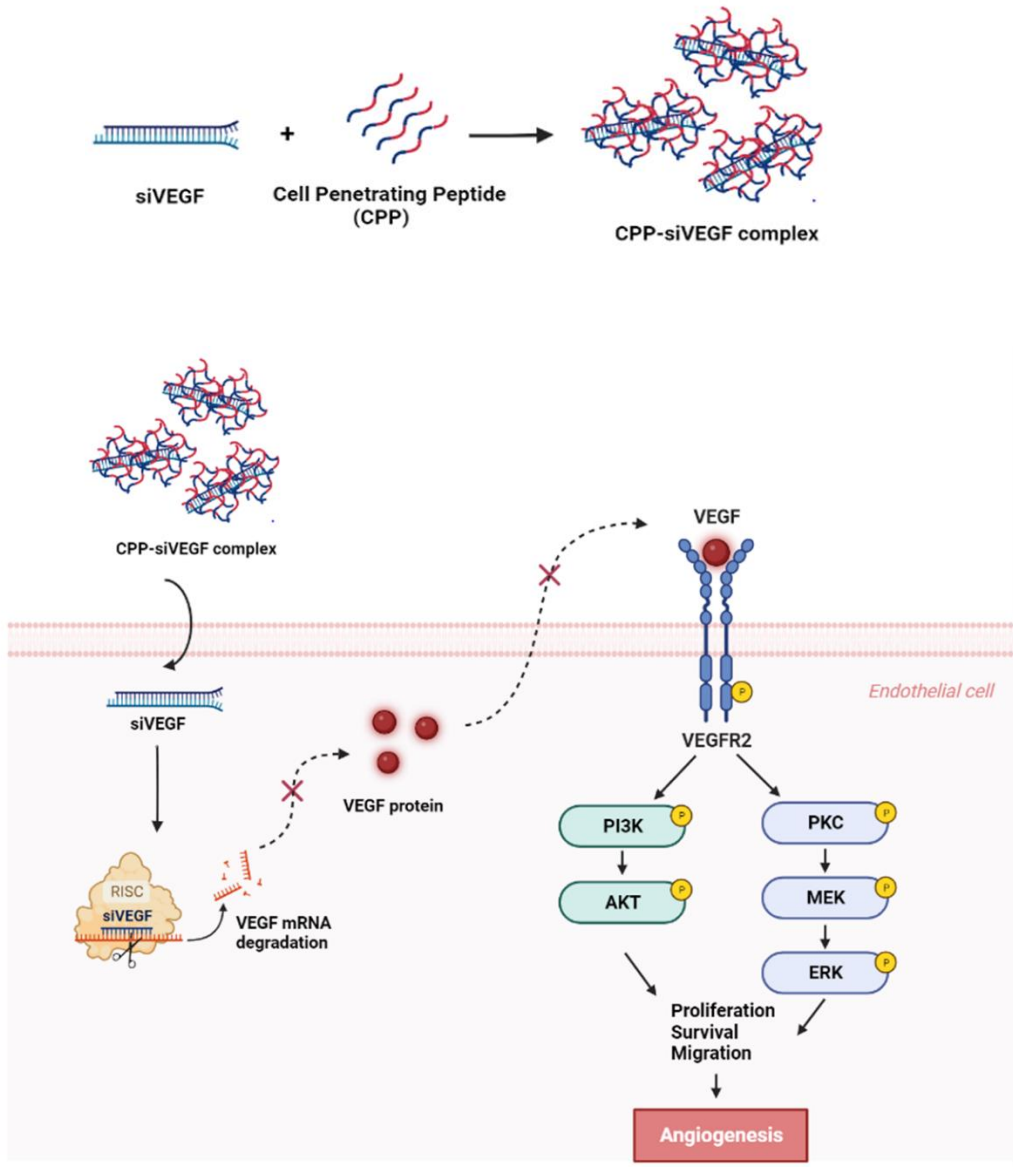

Figure 10. Schema illustrating the mechanism of angiogenesis inhibition in HUVECs by a novel CPP-siVEGF complex. This schema was created with BioRender.com.

DISCUSSION

In this study, a novel CPP-siVEGF complex for intracellular delivery of siVEGF was developed and characterized. Without any other cytotoxicity, the complex successfully exhibited cellular uptake of siVEGF and gene silencing in HUVECs. Specific silencing of VEGF mRNA not only significantly reduced the expression of VEGF protein, but also suppressed the migration of endothelial cells and their ability to form new vascular networks through the regulation of the VEGFR2-mediated AKT and ERK signaling pathways. **(Figure 10)**.

The CPP used in this study, Ara27, complexed well with siVEGF through electrostatic interaction. It has been confirmed that Ara27 can be incorporated into various cell lines at low concentrations under short treatment conditions without cytotoxicity [34]. A significant improvement in intracellular uptake was seen with Ara27 compared to commonly used CPPs, such as Tat-protein transduction domain and membrane translocating sequence, without adverse effects on cell viability [35].

The molar ratio is defined as the number of CPPs required for one molecule of siRNA. It is an important factor influencing the stability of the CPP-siRNA complex. In previous study, the siRNA showed improved results in downregulating expression when complexed with amphipathic CPPs in molar ratios above 1:15 [40]. In this study, I found that the bands significantly

shifted when siVEGF was concentrated from a 1:10 to a 1:30 molar ratio with Ara27.

The size of the complex is also one of the important factors in determining the intracellular uptake [41]. To ensure cellular uptake and tissue distribution, and to overcome the risk of cellular toxicity, the size of a complex of CPP and siRNA must be less than 200 nm [42-45]. I used dynamic light scattering (DLS) to measure the average size and size distribution of Ara27-siVEGF complexes [46]. The polydispersity index (PDI) refers to the degree of non-uniformity in complex size distributions. If the PDI value exceeds 0.7, it indicates a very broad complex size distribution in the sample and the DLS technique is probably not suitable for analysis [47, 48]. A value of 0.2 or below is typically considered acceptable for polymer-based nanoparticles [49]. According to my results of the size of the Ara27-siVEGF complexes, the complexes with a molar ratio of 1:10 and 1:20 were measured to be less than 200 nm. However, the complexes with 1:30 were measured with a size distribution larger than 200 nm and a graph with a large fluctuation in the values. As well, the PDI value at 1:30 is higher than 0.35, suggesting that the complex size distribution is highly unstable. It is predicted to be caused by the aggregation of CPPs.

In my prior experiment, siGAPDH was also formed complex with Ara27 at various molar ratios for knockdown of GAPDH. The Ara27-siGAPDH complex only at 1:20 induced significant downregulation of GAPDH mRNA expression, while 1:10 and 1:30 had less effective in GAPDH knockdown in

human dermal fibroblasts [Unpresented data]. Therefore, I primarily used 1:20 ratio complexes to inhibit angiogenesis in HUVECs. On the basis of the ratio, size distribution, and homogeneity of the complex, I determined that the 1:20 complex was the most suitable ratio for delivering siVEGF *in vitro*.

Cationic lipids and polymers are widely used for nucleic acid delivery into cells *in vitro* and *in vivo* [50-52]. However, the clinical applicability of many cationic vectors developed so far has been restricted by their substantial toxicity. There seems to be a relationship between charge and cellular processes, as excess positive charges on the complex surface can interact with cell membranes, and inhibit normal cellular functions and cell survival signaling [53-55]. For *in vivo* applications, cationic lipids are often the cause of acute inflammatory responses. Cationic polymers, such as polyethyleneimine, induce cell necrosis, apoptosis and autophagy [56].

HUVEC, one of primary cells, have been known to be difficult to transfect and vulnerable to the toxic effects of transfection reagents [57, 58]. I used a commercial polymeric transfection reagent, TransITx2, as a positive control for *in vitro* transfection efficiency. Cell viability decreased significantly despite treatment with transfection reagent alone, while Ara27 maintained viability above 90% in both Ara27 alone and complex treatments. Furthermore, the fluorescence intensity of the intracellularly internalized siVEGF delivered by Ara27 was similar to that of the transfection agent. The results of my experiments indicate that Ara27 might be suitable for siRNA delivery *in vitro* without cytotoxicity concerns.

The endothelial cell migration driven by VEGF is an essential step of angiogenesis [59]. In this study, I elucidated that HUVEC migration was suppressed by Ara27-siVEGF complex. This might be associated with cytoskeletal function, which is essential for modulating cell motility. In the process of angiogenesis, tube formation is highly dependent on the migration of endothelial cells [60]. My data showed that the Ara27-siVEGF complex limited endothelial cell migration and tube formation, further confirming its remarkable inhibitory function on angiogenesis.

As a major signaling pathway in angiogenesis and cell survival, VEGF binds to VEGFR2, phosphorylating and triggering a cascade of signaling that contributes to angiogenesis, permeability or survival [61, 62]. Numerous VEGFR2 downstream signaling mediators, such as AKT and ERK, have also been found to regulate endothelial cell survival and proliferation [63, 64]. According to my results, the Ara27-siVEGF complex inhibits angiogenesis by decreasing the phosphorylation of VEGFR2, AKT and ERK, but does not change their total form levels.

In summary, my results indicate that the Ara27 is a promising candidate for delivering siVEGF. The Ara27-siVEGF complex in the appropriate ratio efficiently delivered siVEGF to HUVECs, resulting in decreased VEGF mRNA and protein expression without inducing cytotoxicity. In addition, the Ara27-siVEGF complex inhibited angiogenesis by suppressing VEGFR2-mediated AKT and ERK phosphorylation. These results also support that CPP is one of the effective therapeutic approaches for siRNA delivery.

Furthermore, CPPs can be suggested as a very potent drug delivery system *in vivo* due to their lower cytotoxicity compared to well-known transfection reagents.

REFERENCES

1. Folkman, J., *Angiogenesis.* Biology of endothelial cells, 1984: p. 412-428.
2. Carmeliet, P., *Angiogenesis in health and disease.* Nat Med, 2003. **9**(6): p. 653-60.
3. Carmeliet, P. and R.K. Jain, *Angiogenesis in cancer and other diseases.* Nature, 2000. **407**(6801): p. 249-57.
4. Folkman, J., *Angiogenesis in cancer, vascular, rheumatoid and other disease.* Nat Med, 1995. **1**(1): p. 27-31.
5. Kopec, M. and H. Abramczyk, *The role of pro- and antiangiogenic factors in angiogenesis process by Raman spectroscopy.* Spectrochim Acta A Mol Biomol Spectrosc, 2022. **268**: p. 120667.
6. Saharinen, P., et al., *VEGF and angiopoietin signaling in tumor angiogenesis and metastasis.* Trends Mol Med, 2011. **17**(7): p. 347-62.
7. Ansari, M.J., et al., *Cancer combination therapies by angiogenesis inhibitors; a comprehensive review.* Cell Commun Signal, 2022. **20**(1): p. 49.
8. Sennino, B. and D.M. McDonald, *Controlling escape from angiogenesis inhibitors.* Nat Rev Cancer, 2012. **12**(10): p. 699-709.
9. Paz-Ares, L.G., et al., *Phase III, randomized, double-blind, placebo-controlled trial of gemcitabine/cisplatin alone or with sorafenib for the first-line treatment of advanced, nonsquamous non-small-cell lung cancer.* J Clin Oncol, 2012. **30**(25): p. 3084-92.
10. des Guetz, G., et al., *Cardiovascular toxicity of anti-angiogenic drugs.* Target Oncol, 2011. **6**(4): p. 197-202.
11. Elice, F. and F. Rodeghiero, *Side effects of anti-angiogenic drugs.* Thromb Res, 2012. **129 Suppl 1**: p. S50-3.

12. Bodnar, R.J., *Anti-Angiogenic Drugs: Involvement in Cutaneous Side Effects and Wound-Healing Complication.* Adv Wound Care (New Rochelle), 2014. **3**(10): p. 635-646.
13. Hannon, G.J., *RNA interference.* Nature, 2002. **418**(6894): p. 244-51.
14. Kim, D.H. and J.J. Rossi, *Strategies for silencing human disease using RNA interference.* Nat Rev Genet, 2007. **8**(3): p. 173-84.
15. Li, J., et al., *A reduction and pH dual-sensitive polymeric vector for long-circulating and tumor-targeted siRNA delivery.* Adv Mater, 2014. **26**(48): p. 8217-24.
16. Nelson, C.E., et al., *Tunable delivery of siRNA from a biodegradable scaffold to promote angiogenesis in vivo.* Adv Mater, 2014. **26**(4): p. 607-14, 506.
17. Castanotto, D. and J.J. Rossi, *The promises and pitfalls of RNA-interference-based therapeutics.* Nature, 2009. **457**(7228): p. 426-33.
18. Watts, J.K., G.F. Deleavey, and M.J. Damha, *Chemically modified siRNA: tools and applications.* Drug discovery today, 2008. **13**(19-20): p. 842-855.
19. Dong, Y., D.J. Siegwart, and D.G. Anderson, *Strategies, design, and chemistry in siRNA delivery systems.* Adv Drug Deliv Rev, 2019. **144**: p. 133-147.
20. Zheng, D., et al., *Topical delivery of siRNA-based spherical nucleic acid nanoparticle conjugates for gene regulation.* Proc Natl Acad Sci U S A, 2012. **109**(30): p. 11975-80.
21. Yin, H., et al., *Non-viral vectors for gene-based therapy.* Nat Rev Genet, 2014. **15**(8): p. 541-55.
22. Milletti, F., *Cell-penetrating peptides: classes, origin, and current landscape.* Drug Discov Today, 2012. **17**(15-16): p. 850-60.
23. Lindgren, M., et al., *Cell-penetrating peptides.* Trends Pharmacol Sci, 2000. **21**(3): p. 99-103.

24. Allolio, C., et al., *Arginine-rich cell-penetrating peptides induce membrane multilamellarity and subsequently enter via formation of a fusion pore.* Proc Natl Acad Sci U S A, 2018. **115**(47): p. 11923-11928.
25. Borrelli, A., et al., *Cell Penetrating Peptides as Molecular Carriers for Anti-Cancer Agents.* Molecules, 2018. **23**(2).
26. Ye, J., et al., *High-yield synthesis of monomeric LMWP (CPP)-siRNA covalent conjugate for effective cytosolic delivery of siRNA.* Theranostics, 2017. **7**(9): p. 2495.
27. Crombez, L., et al., *A new potent secondary amphipathic cell-penetrating peptide for siRNA delivery into mammalian cells.* Mol Ther, 2009. **17**(1): p. 95-103.
28. Lundberg, P., et al., *Delivery of short interfering RNA using endosomolytic cell-penetrating peptides.* Faseb j, 2007. **21**(11): p. 2664-71.
29. Fei, L., et al., *The influence of net charge and charge distribution on cellular uptake and cytosolic localization of arginine-rich peptides.* J Drug Target, 2011. **19**(8): p. 675-80.
30. Bartz, R., et al., *Effective siRNA delivery and target mRNA degradation using an amphipathic peptide to facilitate pH-dependent endosomal escape.* Biochemical Journal, 2011. **435**(2): p. 475-487.
31. Langlet-Bertin, B., et al., *Design and evaluation of histidine-rich amphipathic peptides for siRNA delivery.* Pharm Res, 2010. **27**(7): p. 1426-36.
32. Zaro, J.L., et al., *Nuclear localization of cell-penetrating peptides is dependent on endocytosis rather than cytosolic delivery in CHO cells.* Molecular pharmaceutics, 2009. **6**(2): p. 337-344.

33. Mo, R.H., J.L. Zaro, and W.C. Shen, *Comparison of cationic and amphipathic cell penetrating peptides for siRNA delivery and efficacy.* Mol Pharm, 2012. **9**(2): p. 299-309.
34. Kim, M., et al., *Cellular internalization effect of Ara27 in various cell lines.* Journal of Animal Reproduction and Biotechnology, 2022. **37**(4): p. 239-245.
35. Min, S., et al., *Newly synthesized peptide, Ara-27, exhibits significant improvement in cell-penetrating ability compared to conventional peptides.* Biotechnology Progress, 2020. **36**(5): p. e3014.
36. Zuo, L., et al., *A siRNA targeting vascular endothelial growth factor-A inhibiting experimental corneal neovascularization.* Curr Eye Res, 2010. **35**(5): p. 375-84.
37. Ryoo, N.K., et al., *Therapeutic effects of a novel siRNA-based anti-VEGF (siVEGF) nanoball for the treatment of choroidal neovascularization.* Nanoscale, 2017. **9**(40): p. 15461-15469.
38. Chung, J.Y., et al., *Enhanced Systemic Anti-Angiogenic siVEGF Delivery Using PEGylated Oligo-d-arginine.* Mol Pharm, 2017. **14**(9): p. 3059-3068.
39. Carpentier, G., et al., *Angiogenesis Analyzer for ImageJ - A comparative morphometric analysis of "Endothelial Tube Formation Assay" and "Fibrin Bead Assay".* Sci Rep, 2020. **10**(1): p. 11568.
40. Pärnaste, L., et al., *The Formation of Nanoparticles between Small Interfering RNA and Amphipathic Cell-Penetrating Peptides.* Mol Ther Nucleic Acids, 2017. **7**: p. 1-10.
41. Zhang, S., H. Gao, and G. Bao, *Physical Principles of Nanoparticle Cellular Endocytosis.* ACS Nano, 2015. **9**(9): p. 8655-71.
42. Reischl, D. and A. Zimmer, *Drug delivery of siRNA therapeutics: potentials and limits of nanosystems.* Nanomedicine, 2009. **5**(1): p. 8-20.

43. van Asbeck, A.H., et al., *Molecular parameters of siRNA--cell penetrating peptide nanocomplexes for efficient cellular delivery.* ACS Nano, 2013. **7**(5): p. 3797-807.
44. Kulkarni, S.A. and S.S. Feng, *Effects of particle size and surface modification on cellular uptake and biodistribution of polymeric nanoparticles for drug delivery.* Pharm Res, 2013. **30**(10): p. 2512-22.
45. Faraji, A.H. and P. Wipf, *Nanoparticles in cellular drug delivery.* Bioorg Med Chem, 2009. **17**(8): p. 2950-62.
46. Hallett, F.R., *Particle size analysis by dynamic light scattering.* Food research international, 1994. **27**(2): p. 195-198.
47. Bera, B., *Nanoporous silicon prepared by vapour phase strain etch and sacrificial technique.* Int. J. Comput. Appl, 2015. **975**: p. 8887.
48. Worldwide, M.I., *Dynamic light scattering, common terms defined.* Inform white paper. Malwern Instruments Limited, 2011. **2011**: p. 1-6.
49. Clarke, S., *Development of hierarchical magnetic nanocomposite materials for biomedical applications*. 2013, Dublin City University.
50. Xu, L. and T. Anchordoquy, *Drug delivery trends in clinical trials and translational medicine: challenges and opportunities in the delivery of nucleic acid-based therapeutics.* J Pharm Sci, 2011. **100**(1): p. 38-52.
51. Maurer, N., et al., *Spontaneous entrapment of polynucleotides upon electrostatic interaction with ethanol-destabilized cationic liposomes.* Biophys J, 2001. **80**(5): p. 2310-26.
52. Smyth Templeton, N., *Cationic liposomes as in vivo delivery vehicles.* Curr Med Chem, 2003. **10**(14): p. 1279-87.
53. Gao, X., et al., *The association of autophagy with polyethylenimine-induced cytotoxity in nephritic and hepatic cell lines.* Biomaterials, 2011. **32**(33): p. 8613-8625.

54. Felgner, J.H., et al., *Enhanced gene delivery and mechanism studies with a novel series of cationic lipid formulations.* Journal of Biological chemistry, 1994. **269**(4): p. 2550-2561.
55. Kafil, V. and Y. Omidi, *Cytotoxic impacts of linear and branched polyethylenimine nanostructures in a431 cells.* BioImpacts: BI, 2011. **1**(1): p. 23.
56. Lv, H., et al., *Toxicity of cationic lipids and cationic polymers in gene delivery.* Journal of controlled release, 2006. **114**(1): p. 100-109.
57. van Beijnum, J.R., E. van der Linden, and A.W. Griffioen, *Angiogenic profiling and comparison of immortalized endothelial cells for functional genomics.* Exp Cell Res, 2008. **314**(2): p. 264-72.
58. Colombo, M.G., et al., *Differential ability of human endothelial cells to internalize and express exogenous DNA.* Cardiovasc Drugs Ther, 2001. **15**(1): p. 25-9.
59. Lamalice, L., F. Le Boeuf, and J. Huot, *Endothelial cell migration during angiogenesis.* Circ Res, 2007. **100**(6): p. 782-94.
60. Nacev, B.A. and J.O. Liu, *Synergistic inhibition of endothelial cell proliferation, tube formation, and sprouting by cyclosporin A and itraconazole.* PLoS One, 2011. **6**(9): p. e24793.
61. Kowanetz, M. and N. Ferrara, *Vascular endothelial growth factor signaling pathways: therapeutic perspective.* Clin Cancer Res, 2006. **12**(17): p. 5018-22.
62. Takahashi, H. and M. Shibuya, *The vascular endothelial growth factor (VEGF)/VEGF receptor system and its role under physiological and pathological conditions.* Clinical science, 2005. **109**(3): p. 227-241.
63. Solorzano, C.C., et al., *In vivo intracellular signaling as a marker of antiangiogenic activity.* Cancer research, 2001. **61**(19): p. 7048-7051.

64. Kilic, E., et al., *The phosphatidylinositol-3 kinase/Akt pathway mediates VEGF's neuroprotective activity and induces blood brain barrier permeability after focal cerebral ischemia.* FASEB journal, 2006. **20**(8): p. 1185.

국문초록

새로운 세포 투과 펩타이드-siVEGF 복합체를 이용한 인간 탯줄 정맥 내피세포의 혈관 신생 억제

김 민 서
협동과정 유전공학 전공
서울대학교 자연과학대학원
(지도교수: 노상호, D.V.M., Ph.D.)

혈관 내피세포 성장인자(VEGF)에 의해 매개되는 혈관 신생은 상처 치유, 염증성 질환, 심혈관 질환, 안구 질환, 특히 종양 성장에 핵심적인 역할을 한다. 따라서 혈관 신생을 조절하는 것은 질병을 치료할 수 있는 유망한 후보이며 VEGF 와 그 수용체를 표적으로 하는 치료제 개발을 위한 연구들이 수행되고 있다. RNA 간섭(RNAi)은 질병 치료를 위한 효과적인 수단이지만, 효율적인 소형 간섭 RNA(siRNA) 전달 시스템의 부재로 인해 그 적용이 제한되어 왔다. 본 연구는 양친매성 세포 투과 펩타이드인 Ara27 이 VEGF siRNA(siVEGF)와 복합체를 형성하여 효과적인 siVEGF 전달체임을 입증하고자 연구를 수행하였다.

Ara27-siVEGF 복합체는 인간 제대 정맥 내피세포에 세포독성을 야기하지 않으면서 효과적으로 siVEGF 를 전달하였고, 특히 VEGF 의 mRNA 및 단백질 수준을 모두 하향 조절하였다. 또한, 혈관 신생의 지표가

될 수 있는 인간 제대 정맥 내피세포의 상처치유를 위한 세포 이동과 혈관 튜브 형성이 감소되는 것을 확인하였다. 이러한 기작은 VEGFR2, AKT 및 ERK 신호경로의 인산화를 감소시킴으로써 발생되는 메커니즘을 확인하였다. 결과적으로, 인간 탯줄 정맥 내피세포의 혈관 신생 억제는 새로운 세포 투과 펩타이드−siVEGF 복합체로 확인하였다. 이러한 결과들은 Ara27 이 세포독성을 유발하지 않고 효율적인 siRNA 전달체의 잠재적 후보임을 시사한다.

주요어: 혈관 신생, 세포 투과성 펩타이드, 인간 제대 정맥 내피세포,
혈관 내피세포 성장인자 소형간섭 RNA, 약물 전달 시스템

학번: 2021−29018